Optical properties and electrical characterization of *p*-type ZnO thin films prepared by thermally oxiding Zn_3N_2 thin films

B.S. Li
Key Laboratory of Excited State Processes, Chinese Academy of Sciences, Changchun Institute of Optics, Fine Mechanics and Physics, Chinese Academy of Sciences 130022, People's Republic of China

Y.C. Liu[a)]
Key Laboratory of Excited State Processes, Chinese Academy of Sciences, Changchun Institute of Optics, Fine Mechanics and Physics, Chinese Academy of Sciences 130022, People's Republic of China, and Institute of Theoretical Physics, Northeast Normal University, Changchun 130024, People's Republic of China

Z.Z. Zhi
Institute of Theoretical Physics, Northeast Normal University, Changchun 130024, People's Republic of China

D.Z. Shen, Y.M. Lu, J.Y. Zhang, and X.W. Fan
Key Laboratory of Excited State Processes, Chinese Academy of Sciences, Changchun Institute of Optics, Fine Mechanics and Physics, Chinese Academy of Sciences 130022, People's Republic of China

R.X. Mu and Don O. Henderson
Chemical Physics Laboratory, Department of Physics, Fisk University, Nashville, Tennessee 37208

(Received 27 May 2002; accepted 30 October 2002)

In this paper, we report a simple method for preparing *p*-type ZnO thin films by thermal oxidization of Zn_3N_2 thin films. The Zn_3N_2 films were grown on fused silica substrates by using plasma-enhanced chemical vapor deposition from a $Zn(C_2H_5)_2$ and NH_3 gas mixture. The Zn_3N_2 film with a cubic antibixbyite structure transformed to ZnO:N with a hexagonal structure as the annealing temperature reached 500 °C. When the annealing temperature reached 700 °C, a high-quality *p*-type ZnO film with a carrier density of 4.16×10^{17} cm^{-3} was obtained, for which the film showed a strong near-band-edge emission at 3.30 eV without deep-level emission, and the full width at half-maximum of the photoluminescence spectrum was 120 meV at room temperature. The origin of the ultraviolet band was the overlap of free exciton and the bound exciton. The N concentration was as high as 10^{21} cm^{-3}, which could be controlled by adjusting the parameters of the annealing processes.

As a wide band gap semiconductor with a large excitonic binding energy of 60 meV, zinc oxide (ZnO) (E_g = 3.4eV) has been recognized as a promising material for use in ultraviolet (UV) light emission devices and laser diodes. Recently, the optically pumped stimulated emission of ZnO thin films has been reported,[1–7] making it a hotspot in opto-electronic materials and devices, as a promising candidate for realizing the short-wavelength light-emitting devices (LEDs). To realize this device, an important issue is the fabrication of *p*-type ZnO with a low resistance. However, it is difficult to prepare *p*-type ZnO due to the self-compensated effect in wide band gap semiconductors.

ZnO is naturally a strong *n*-type material. It can be doped into *n*-type to very low resistance using group III elements,[8] while it is difficult to obtain an efficient *p*-type doping. The report in Ref. 6 has demonstrated that nitrogen is a good *p*-type dopant for ZnO. However, it has been reported that the ZnO thin films deposited in pure N_2 plasma were actually *n*-type.[9,10] It is difficult to obtain *p*-type ZnO, which has been attributed to the self-compensation by native defects and low solublity for N in ZnO due to its high formation energy.[11] The "co-doping" method was an effective way to prepare *p*-type

a)Address all correspondence to this author.
e-mail: ycliu@nenu.edu.cn

ZnO, verified by theoretical calculation and experiments, leading to the enhancement of acceptor doping.[12–14] However, its reproducibility is much lower, which results from the difficulty in controlling the amounts and its distribution in the ZnO thin films, making it unsuitable for practical application.[11,15]

Because the chemical activity of oxygen is higher than that of N, Zn preferentially combines with O rather than with N. Thus it is difficult for N to be incorporated into ZnO films, even though N is activated by plasma.[9,10] However, the thermal oxidation of Zn_3N_2 method can overcome this problem, where the low solubility of the N acceptor in ZnO can be solved. Here, the N atoms in Zn_3N_2 film are replaced by O atoms by thermal annealing in an oxygen ambient. The residual N atoms in the newly formed ZnO:N film will act as acceptors to be controlled by annealing processes. The main advantages of this method are to incorporate heavy N into ZnO thin film and also to make the N atoms in O sites.

Zn_3N_2 with a cubic antibixbyite structure (CAS) is taken as an incomplete cubic close packing of zinc ions. The zinc atoms occupy three-fourths of the fluorine positions in the CaF_2 structure, and each nitrogen atom has four closest zinc atoms around it.[16] Zn_3N_2 is also an *n*-type semiconductor with a direct band gap; however, its band gap is still disputed.[16,17] The N in Zn_3N_2 can be replaced by O, leading to the formation of ZnO with a hexagonal structure. If we control the annealing condition, the residual nitrogen atoms will become acceptors in ZnO:N films. As a result, we can obtain *p*-type ZnO thin films by a simple method. Success in easily realizing *p*-type ZnO will undoubtedly widen the range of applications for ZnO to a great extent.

For this communication, we deposited Zn_3N_2 thin films at a low temperature of 140 °C on fused silica by employing the plasma-enhanced chemical vapor deposition (PECVD) method. We also report an original method for achieving *p*-type ZnO thin film with high carrier density and good luminescent properties by the thermal oxidation of Zn_3N_2 films.

Zn_3N_2 thin films with a thickness of 1 μm were deposited on the fused silica substrate at a low temperature of 140 °C by employing the PECVD system, which was introduced previously.[18] The substrate was chemically etched by a standard Radio Corporation of American cleaning process before film deposition.[18] Diethylzinc (DEZ), NH_3, and high-purity H_2 were the zinc source, N source, and carrier gas, respectively. The growing pressure was 100 Pa, and the DEZ was contained in a well-cooled stainless-steel cylinder and was kept at 30 °C by a CW-1 type fine-controlled semiconductor temperature device (Changchun Institute of Physics, Changchun, People's Republic of China). After deposition, the sample was divided into small pieces and placed in a thermal furnace. Thermal oxidation was carried out in an oxygen ambient with different annealing temperatures from 300 to 800 °C for 1 h. The crystal structure of thin films was determined by x-ray diffraction (XRD). The Au–Cr metal as an electrode was thermally vaporized onto the films and rapid annealed at 300 °C for 1 min. The electronic properties of films were studied by the Van der Pauw method. The N concentration was evaluated by x-ray photoelectron spectroscopy (XPS; VG ESCALAB MK II XPS, VG Co., East Grinstead, United Kingdom). The photoluminescence (PL) of films was measured by a He–Cd laser of 325-nm line with a output power of 30 mW at room temperature. The emission signals of the PL were detected by a charge couple device in a backscattering configuration.

Figure 1 shows the θ-2θ XRD patterns of the films annealed at different temperatures. For comparison, the XRD scan for the as-deposited film is also shown in Fig. 1(a). In Fig. 1(a), main diffraction peak corresponds to the Zn_3N_2 (321) diffraction (the lattice constant is evaluated to be $a = 9.791$ Å, which is in agreement with the previously reported value[16]); however, unexpected secondary (100) and (110) peaks of ZnO were also observed. This shows that the Zn_3N_2–ZnO mixed film formed. Maybe this was due to the residual oxygen in the reaction chamber. The sample annealed at 300 and

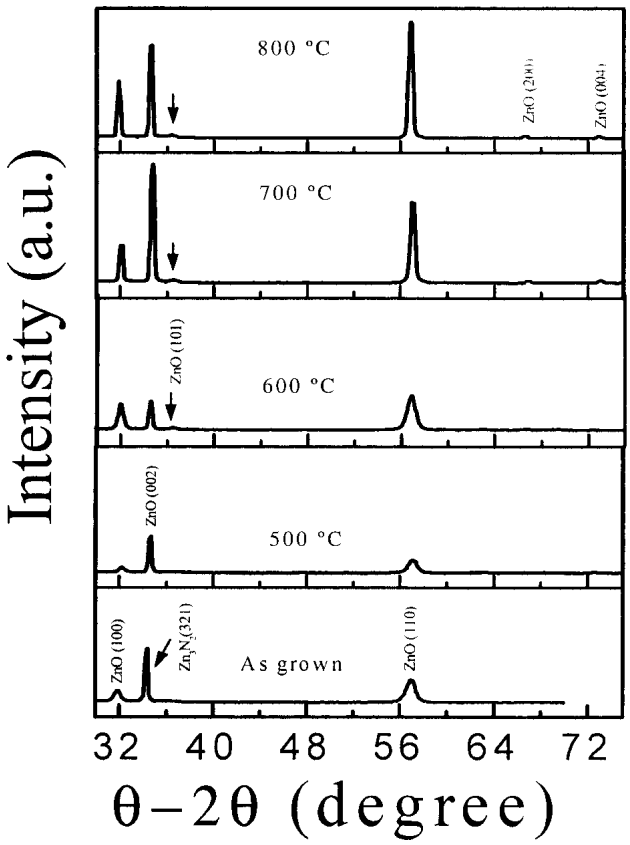

FIG. 1. XRD spectra of films: (a) as-deposited and (b-e) annealed at 500, 600, 700, and 800 °C, respectively.

400 °C did not show obvious changes compared with the as-deposited film, except a weak ZnO (101) peak. When the as-grown film was annealed at 500 °C in an O_2 ambient for 1 h, the Zn_3N_2 transformed from Zn_3N_2 to ZnO entirely. The XRD patterns indicate that the obtained ZnO thin films possessed a polycrystalline hexagonal wurtzite structure (HWS) without preferred orientation. With increasing annealing temperature, the intensities of the main peaks increased, and the full width at half-maximum narrowed, thus improving the crystal quality. No evidence of CAS ZnO was found in the XRD patterns of the samples oxidized at 500, 600, 700, and 800 °C, indicating that the N sites in the CAS Zn_3N_2 were not simply replaced by oxygen during the thermal annealing process. From the evolution of the XRD, we think structural phase changes happened after the adsorbed and diffused O atoms substituted for the N atoms. The oxygen atoms adsorbed and diffused into the Zn_3N_2 matrix via interstitial sites and bonded to Zn due to its larger electronegativity (3.50) comparing to N atom (3.04); as a rusult, part of the N atoms were replaced by oxygen atoms. For the annealing temperature lower than 500 °C, the oxide processes occurred at the surface of films, as confirmed by XRD results. With the increasing of the annealing temperature, the oxygen atoms can diffuse into the films and more N atoms were replaced by O atoms, leading to structural phase change from CAS to HWS, resulting in the formation of ZnO:N thin films. The residual N concentration can be affected by the annealing temperature, the annealing time, and the ambience, as shown by XPS.

The electrical measurements, including resistivity, Hall coefficient, carrier density and mobility, were performed with a Van der Pauw four-point probe system with micro miniature refrigerators technology. All measurements were conducted at 300 K. The temperature variance was less than 0.1 K. The typical current used for the measurements was approximately 3 nA and the magnetic field was 2500 G. The Au–Cr metal used as an electrode was thermally vaporized onto the films. No significant deviation was observed from the both contacts. In addition, low-temperature thermal annealing and preliminary testing suggested that all four contacts were Ohmic. The image in Fig. 2 is the surface *I-V* relation of ZnO thin films annealed at 700 and 800 °C. For linear dependence of *I-V* characteristics, the Ohmic contact between ZnO:N and the Au–Cr electrode are fairly confirmed. Electrical transport properties of ZnO films are summarized in Table I. The samples that are as grown and oxided at 300 and 400 °C are *n*-type with the decrease of carrier density from 10^{15} to 10^{12} cm^{-3}. On the contrary, for the samples annealed at 600 and 700 °C, respectively, the Hall coefficient was inverted to positive from negative, indicating a hole-dominant transport effect. The carrier densities of hole are 1.2×10^{14} and 4.16×10^{17} cm^{-3}, respectively. With the increase of annealing temperature, more N-acceptors in ZnO will be activated, accompanying with a decrease the density of donor-like defects. So the density of electron will decrease with increasing annealing temperature. At last, the density of acceptor will be dominant, and the ZnO was inverted from *n*-type to *p*-type. However, as the annealing temperature further (800 °C) increases, the residual N atoms

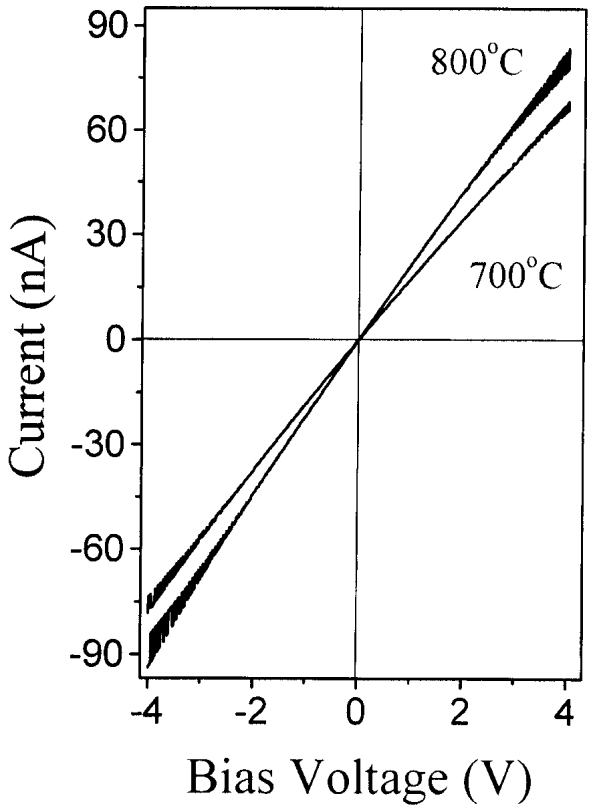

FIG. 2. Surface *I-V* characteristics of ZnO thin films annealed at 600, 700, and 800 °C. The dependence of current on the voltage shows a straight line, which indicates the formation of Ohmic contact between the electrode and ZnO films.

TABLE I. Summary of electrical properties of samples annealed at different temperatures in oxygen ambient.

Annealing temperature	Resistivity (Ohm cm)	Mobility (cm^2/Vs)	Density (cm^{-3})	Hall coeff. (cm^3/Coul)	Carriers	N concentration (cm^3)
As grown	84.02	39.72	1.87×10^{15}	−3337.3	*e*	
600 °C	14980	3.52	1.2×10^{14}	+52768	*h*	6.87×10^{21}
700 °C	153.05	0.098	4.16×10^{17}	+15.02	*h*	6.78×10^{21}
800 °C	66	56.8	1.67×10^{15}	−3747	*e*	5.48×10^{21}

will be further replaced by the oxygen atoms, leading to reconversion of *p*-type ZnO back to *n*-type. The N concentration in the films annealed at 600, 700, and 800 °C are 6.87×10^{21}, 6.78×10^{21}, and 5.48×10^{21} cm^{-3}, respectively, estimated by XPS. Shown in Fig. 3 is a typical XPS spectrum of N 1*s* centered at 398.33 eV, which corresponds to the N–Zn bond.[19] N concentrations are calculated by using the formula:

$$C_N = \frac{\frac{S_N}{asf_N}}{\frac{S_N}{asf_N} + \frac{S_O}{asf_O} + \frac{S_{Zn}}{asf_{Zn}}} \times 10^{23} \quad ,$$

where *S* is the integral intensity of peak for N, Zn, and O elements, and *asf* is the atomic scattering factor. The N concentration is two orders higher than the up-to-date report using the co-doping method.[20] The N concentration decreases with increasing annealing temperature. The film with N concentration as high as 5.48×10^{21} cm^{-3} still shows the *n*-type, meaning the strong self-compensation occurred in ZnO. At room temperature, the ionization rate (IA) for N defects is estimated to be 10^{-4}, deduced from the ratio of the hole density to the N concentration. According to its ionization rate, the active energy of N is estimated about 252 meV above the valence bands by using the formula, IA $\propto \exp(-\delta E/kT)$. This level is slightly lower than the calculation by first-principles.[11] Generally, the mobility of the carrier is mainly determined by both ionized impurity scattering and grain boundary scattering in polycrystalline semiconductor films. Here the resistivity of *p*-type ZnO is still a little high for application in devices such as LEDs. In our experiment, we found the properties of ZnO are closely related to the parameters, such as the annealing temperature, thermal oxidation time, the annealing method, and Zn_3N_2 crystal quality, which are still not identified clearly. It is also necessary to further study the relationships between the properties, in particular the electrical properties, with the parameters. We believe that the properties of *p*-type ZnO can be improved by further optimizing the experiment parameters. The V group elements such as N, As, and P are very good *p*-type dopants for ZnO, demonstrated by other experiments.[21,22] Here, we expect that *p*-type ZnO can also be obtained for thermal oxidation of other II-V compounds, such as Zn_3As_2 and Zn_3P_2. In particular, since the Zn_3P_2 is a natural *p*-type semiconductor,[17] maybe it is much easier to obtain *p*-type ZnO with high hole density. The hole density of *p*-type ZnO can also be expected to increase by the oxidation of Zn_3V_2 compound grown on GaAs or InP substrate, utilizing the diffusion of V elements from the substrate into the epitaxy due to their larger evaporating pressure.[23] The diffusion effect can compensate for the excess loss of V group elements in the epitaxy during the thermal oxidation. To confirm the electrical characterization, a Zn_3N_2 thin film was grown on the *n*-type Si substrates. Then the Zn_3N_2 sample was separated into small pieces and annealed at different temperatures. The *p*-ZnO was obtained at optimizing condition. A rectifying *p–n* junction behavior can be observed from the *p*-ZnO/*n*-Si heterojunction, meaning a *p*-ZnO has been fabricated by thermal Zn_3N_2 thin films. These results were also confirmed by Seebeck coefficient measurement. These will be reported in detail in another paper.[24]

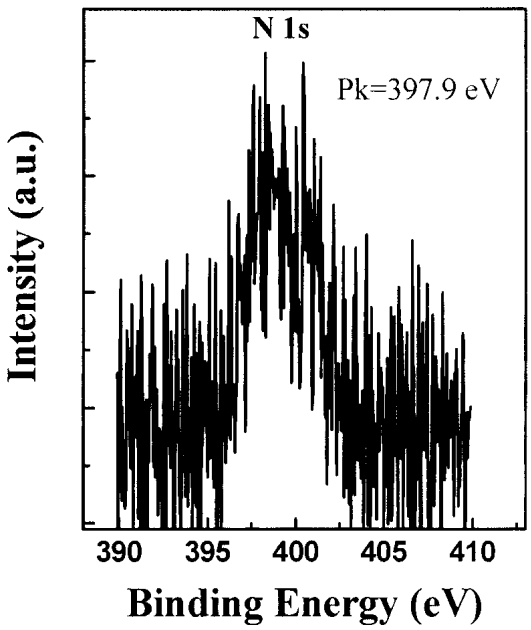

FIG. 3. A typical N 1*s* spectrum of XPS analysis for ZnO:N prepared by thermal oxidizing Zn_3N_2 at 600 °C in an oxygen ambient.

Figure 4 shows the room-temperature PL spectra of ZnO annealed at different temperatures. The films oxidized at 300, 400, and 500 °C give nearly no emission (not shown). An onset of UV emission was observed at the annealing temperature of 600 °C. A strong UV emission band at 3.30 eV without deep level emission was shown in the film at the annealing temperature of 700 °C. There were lots of defects, such as oxygen vacancies, Zn interstitial in the films for the transformation of ZnS to ZnO induced from thermal oxidation process.[25] At low annealing temperature, the oxidization process takes place, and Zn_3N_2 transforms to ZnO:N but with poor quality. Due to the existence of quantities of defects, no light emission is observed for the samples annealed at 500 °C. When the annealing temperature is further increased, the ZnO crystallinity will grow, resulting in better crystal quality and strong UV emission. This is also consistent with the evolution of the XRD peak width at different temperatures. The origin of the UV band located at 3.30 eV at room temperature is from the recombination of free exciton.[26] A shoulder at the low energy

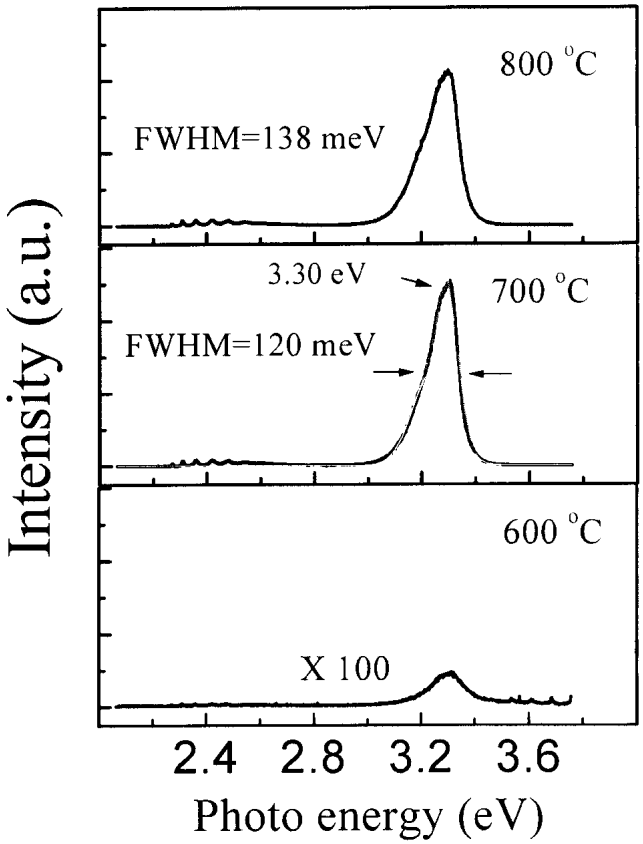

FIG. 4. PL spectra of films annealed at 600, 700, and 800 °C, respectively. A strong UV emission at 3.30 eV without deep-level emission is observed. The full width at half-maximum of the PL spectrum is 120 meV at room temperature.

side is observed around 3.241 eV, which is assumed to be exciton bound at the neutral acceptor. This has been investigated by measuring the temperature dependent PL spectra (explained below). However, the optical properties of the film annealed at 800 °C show the same characterization. We also think the luminescence is from the overlap of the free exciton and bound exciton due to the existence of high N concentration in this film. However, as the annealing temperature increases, more structure defects will be generated, resulting in the increase of the full width at half-maximum of the PL spectra from 120 to 138 meV, as shown in Fig. 4.

To understand the origin of the UV band, we studied the PL of *p*-ZnO annealed at 700 °C at various temperature. As shown in Fig. 5, the UV band was resolved as five separate peaks at 3.368, 3.312, 3.239, 3.170, and 3.100 eV at 80.5 K. Judging from its energy position, the emission line located at 3.368 eV (assigned P1) is from A-exciton emission for it is in excellent agreement with 3.369 eV from A-exciton recombination reported by Butkhuzi *et. al.*[27] The P2 emission line, near the emission line of exciton bound to acceptor in ZnO[28] is observed at 3.312 eV, accompanied by 1 LO, 2 LO, and 3 LO replicas at 3.239, 3.170, and 3.100 eV due to their energy

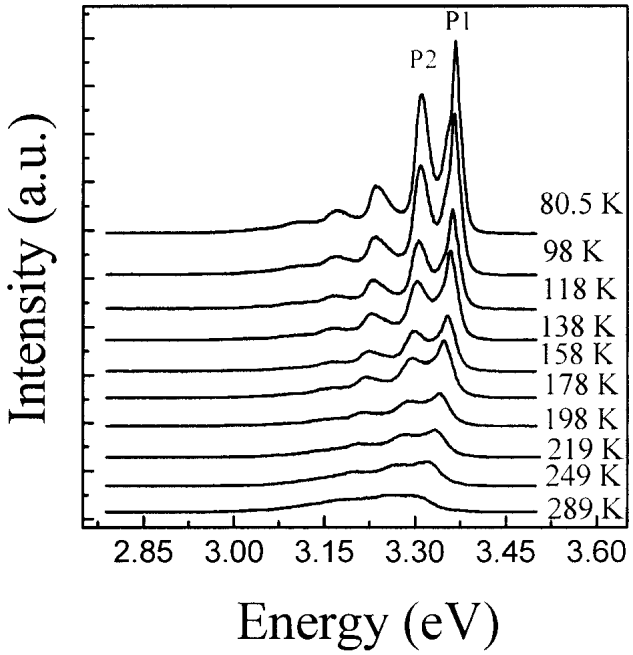

FIG. 5. Temperature-dependent PL spectra of *p*-type ZnO annealed at 700 °C for a temperature of 80–300 K.

differences, which consistent with longitudinal-optical-phonon energy of 72 ± 4 meV. Note that P2 line can only be observed in N-doped ZnO, and this line position also did not change with the excitation power changing. Furthermore, with the decreasing excited power density, the PL intensity ratio of P2 to P1 increases. These features suggest that this line emission can be attributed to bound excitons.[29] For comparison, the PL spectra of the undoped ZnO prepared by using PECVD and the sample annealed at 1000 °C were carried out at 80.5 K, as shown in Fig. 6. The most obvious difference is that the P2 peak nearly disappeared at an annealed temperature of 1000 °C and P2 peak is not observed in the undoped ZnO. So, the P2 peak is most likely associated with N_O. Thus, the reasonable explanation for the 3.312 line is that it is exciton emission bound to neutral N_O-acceptor because it is a *p*-type material with a larger amount of doping N in ZnO. The temperature-dependent PL spectra show that the UV band at room temperature is from the overlap of the free exciton and bound exciton binded by N-acceptor.

In summary, Zn_3N_2 film was successfully prepared by PECVD at low temperatures. Zn_3N_2 was transformed completely into ZnO around 500 °C by thermal oxidation in the oxygen ambient. The *p*-type ZnO with the hole density of 4.16×10^{17} was obtained at the annealing temperature of 700 °C. The doping concentration of N atom reached 10^{21} cm^{-3}. PL spectra showed a strong UV band at 3.30 eV without deep level emission, and the origin of the UV band was the overlap of the free exciton and bound exciton. The extreme difficulty of preparing

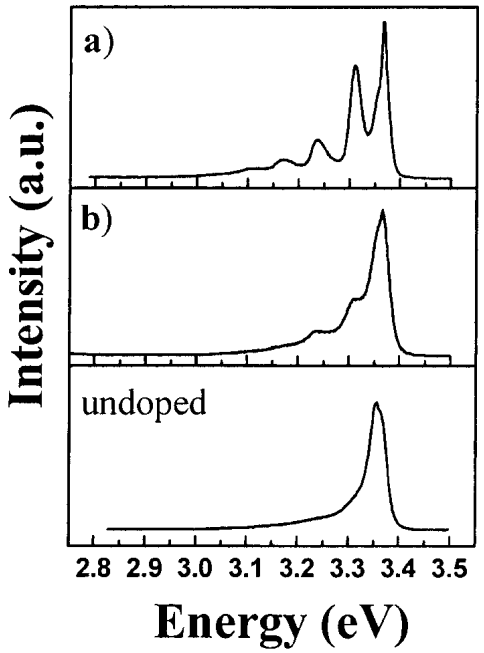

FIG. 6. PL spectra at low temperature of 80.5 K for the three samples, which are annealed at (a) 700 °C and (b) 1000 °C and an undoped, PECVD-grown ZnO film.

p-type ZnO was overcome by a simple method, suggesting that the thermal oxidation of II-V compound provided a new way to prepare *p*-type ZnO. Deposition of intrinsic *n*-type ZnO onto our *p*-type ZnO layer will make it possible to produce a *p–n* junction or *p–i–n* diode. Relevant work is still in progress.

ACKNOWLEDGMENTS

The first author is very grateful to Prof. X.L. Li for his measurements of XPS and calculation of the N concentration. This work was supported by the Program of Chinese Academy of Sciences Hundred Talents, the National Natural Science Foundation of China, the innovation foundation of Changchun Institute of Optics, Fine Mechanics, and Physics, and the Foundation of Excellent Research to Go Beyond the Century of the Ministry of Education of China.

REFERENCES

1. D.C. Reynolds, D.C. Look, and B. Jogai, Solid State Commun. **99,** 873 (1996).
2. D.M. Bagnall, Y.F. Chen, Z. Zhu, T. Yao, S. Koyama, M.Y. Shen, and T. Goto, Appl. Phys. Lett. **70,** 2230 (1997).
3. T.K. Tang, G.K.L. Wong, P. Yu, M. Kawasaki, A. Ohtomo, H. Koinuma, and Y. Segawa, Appl. Phys. Lett. **72,** 3270 (1998).
4. M.H. Huang, S. Mao, H. Feick, H. Yan, Y. Wu, H. Kind, E. Weber, R. Russo, and P. Yang, Science **292,** 1897 (2001).
5. A. Mitra and R.K. Thareja, J. Appl. Phys. **89,** 2025 (2001).
6. R.F. Service, Science **276,** 895 (1997).
7. X.T. Zhang, Y.C. Liu, L.G. Zhang, J.Y. Zhang, Y.M. Lu, D.Z. Shen, W. Xu, G.Z. Zhong, X.W. Fan, and X.G. Kong, Chin. Phys. Lett. **19,** 127 (2002).
8. T. Minami, H. Sato, H. Nanto, and S. Takata, Jpn. J. Appl. Phys. **24,** L781 (1985).
9. Y. Sato and S. Sato, Thin Solid Films **281–282,** 445 (1996).
10. X.Q. Wang, S.R. Yang, J.Z. Wang, M.T. Li, X.Y. Jiang, G.T. Du, X. Liu, and R.P.H. Chang, J. Cryst. Growth **226,** 123 (2001).
11. Y.F. Yan, S.B. Zhang, S.J. Pennycook, and S.T. Pantelides (unpublished).
12. T. Yamamoto and H. Katayama-Yoshida, Jpn. J. Appl. Phys. **38,** L166 (1999).
13. M. Joseph, H. Tabata, and T. Kawai, Jpn. J. Appl. Phys. **38,** L1205 (1999).
14. M. Joseph, H. Tabata, H. Saeki, K. Ueda, and T. Kawai, Physica B **302–303,** 140 (2001).
15. X.L. Guo, H. Tabata, and T. Kawai, J. Cryst. Growth. **223,** 135 (2001).
16. K. Kuriyama, Y. Takahashi, and F. Sunohara, Phys. Rev. B **48,** 2781 (1993).
17. M. Futsuhara, K. Yoshioka, and O. Takai, Thin Solid Films **322,** 274 (1998).
18. B.S. Li, Y.C. Liu, D.Z. Shen, Y.M. Lu, J.Y. Zhang, X.G. Kong, Z.Z. Zhi, and X.W. Fan. J. Vac. Sci. Technol. A **20,** 501 (2002).
19. M. Joseph, H. Tabata, and T. Kawai, Jpn. J. Appl. Phys. **38,** L1025 (1999).
20. A. Tsukazaki, H. Saito, K. Tamura, M. Ohtani, H. Koinuma, M. Sumiya, S. Fuke, T. Fukumura, and M. Kawasaki, Appl. Phys. Lett. **81,** 235 (2002).
21. Y.R. Ryu, S. Zhu, D.C. Look, J.M. Wrobel, H.M. Jeong, and H.W. White, J. Cryst. Growth **216,** 330 (2000).
22. T. Aoki, Y. Hatanaka, and D.C. Look, Appl. Phys. Lett. **76,** 3257 (2000).
23. Y.R. Ryu, W.J. Kim, and H.W. White, J. Cryst. Growth **219,** 419 (2000).
24. D. Wang, Y.C. Liu, J.Y. Zhang, Z.Z. Zhi, D.Z. Shen, Y.M. Lu, and X.W. Fan (unpublished).
25. Y.Z. Yoo, Y. Osaka, T. Fukumura, Z.W. Jin, M. Kawasaki, H. Koimuma, T. Chikyow, P. Ahmet, A. Setoguchi, and S.F. Chichibu, Appl. Phys. Lett. **78,** 616 (2001).
26. M. Joseph, H. Tabata, H. Saeki, K. Ueda, and T. Kawai, Physica B **302–302,** 140 (2001).
27. T.V. Butkuzi, T.G. Chelizde, A.N. Georgobiani, D.L. Jashiashvili, T.G. Khulordava, and B.E. Tsekvava, Phys. Rev. B **58,** 10692 (1998).
28. M.K. Ryu, S.H. Lee, M.S. Jang, G.N. Panin, and T.W. Kang, J. Appl. Phys. **92,** 154 (2002).
29. H.J. Ko, Y.F. Chen, Z. Zhu, T. Yao, I. Kobayashi, and H. Uchiki, Appl. Phys. Lett. **76,** 1905 (2000).